

# Automated next-to-leading order predictions for new physics at the LHC: The case of colored scalar pair production

Céline Degrande,<sup>1</sup> Benjamin Fuks,<sup>2,3</sup> Valentin Hirschi,<sup>4</sup> Josselin Proudom,<sup>5</sup> and Hua-Sheng Shao<sup>2</sup>

<sup>1</sup>*Institute for Particle Physics Phenomenology, Department of Physics Durham University, Durham DH1 3LE, United Kingdom*

<sup>2</sup>*CERN, PH-TH, CH-1211 Geneva 23, Switzerland*

<sup>3</sup>*Institut Pluridisciplinaire Hubert Curien/Département Recherches Subatomiques,*

*Université de Strasbourg/CNRS-IN2P3, 23 Rue du Loess, F-67037 Strasbourg, France*

<sup>4</sup>*SLAC, National Accelerator Laboratory, 2575 Sand Hill Road, Menlo Park, CA 94025-7090, USA*

<sup>5</sup>*Laboratoire de Physique Subatomique et de Cosmologie, Université Grenoble-Alpes, CNRS/IN2P3, 53 Avenue des Martyrs, F-38026 Grenoble Cedex, France*

We present for the first time the full automation of collider predictions matched with parton showers at the next-to-leading accuracy in QCD within non-trivial extensions of the Standard Model. The sole inputs required from the user are the model Lagrangian and the process of interest. As an application of the above, we explore scenarios beyond the Standard Model where new colored scalar particles can be pair produced in hadron collisions. Using simplified models to describe the new field interactions with the Standard Model, we present precision predictions for the LHC within the MADGRAPH5\_aMC@NLO framework.

## I. INTRODUCTION

Motivated by the conceptual issues accompanying the Standard Model, many new physics theories have been developed over the last decades. Most of them exhibit an extended colored sector and related new phenomena are expected to be observable at high-energy hadron colliders such as the LHC. In particular, effects induced by hypothetical colored scalar particles have received special attention from both the ATLAS and CMS collaborations. Many LHC analyses are indeed seeking for the scalar partners of the Standard Model quarks (the squarks) and gluons (the sgluons) that are predicted, for instance, in minimal [1, 2] and non-minimal [3, 4] supersymmetric or in vector-like confining theories [5].

In this context, it is clear that an approach to precision predictions that is fully general in any considered theory is highly desirable, and the MADGRAPH5\_aMC@NLO framework [6] is in a prime position to provide it. Its structure for tackling leading-order (LO) computations has indeed already proved to be very efficient at satisfying the needs of both the theoretical and experimental high energy physics communities. Generalizing this flexibility to the next-to-leading order (NLO) case is however not straightforward, essentially because of the necessity of specifying model-dependent counterterms, including those arising from the renormalization of the Lagrangian. Recent developments [7] in the FEYNRULES package [8] have allowed to overcome this main obstacle and paved the way to the full automation of NLO QCD predictions matched to parton showers for generic theories.

We describe the details of this implementation by working through two specific cases and revisit some LHC phenomenology associated with stops and sgluons in the context of simplified models of new physics [9, 10]. Employing state-of-the-art simulation techniques, we match matrix elements to the NLO in QCD to parton showers and present precision predictions for several kinematical

observables after considering both the production and the decay of the new particles. In more detail, we make use of FEYNRULES to implement all possible couplings of the new fields to quarks and gluons and employ the NLOCT program [7] to generate a UFO module [11] containing, in addition to tree-level model information, the ultraviolet and  $R_2$  counterterms necessary whenever the loop integral numerators are computed in four dimensions, as in MADLOOP [12] that uses the Ossola-Papadopoulos-Pittau (OPP) reduction formalism [13]. This UFO library is then linked to the MADGRAPH5\_aMC@NLO framework which is used, for the first time, for predictions in the context of new physics models featuring an extended colored sector. We focus on the pair production of the new states at NLO in QCD. Their decay is then taken into account separately, at the leading order and with the spin information retained, by means of the MADSPIN [14] and MADWIDTH [15] programs.

In the rest of this paper, we first define simplified models describing stop and sgluon dynamics and detail the renormalization of the effective Lagrangians and the validation of the UFO models generated by NLOCT. Our results follow and consist of total rates and differential distributions illustrating some kinematical properties of the produced new states and their decay products.

## II. BENCHMARK SCENARIOS FOR STOP HADROPRODUCTION

Following a simplified model approach, we extend the Standard Model by a complex scalar field  $\sigma_3$  (a stop) of mass  $m_3$ . This field lies in the fundamental representation of  $SU(3)_c$ , so that its strong interactions are standard and embedded into  $SU(3)_c$ -covariant derivatives. We enable the stop to decay via a coupling to a single top quark and a gauge-singlet Majorana fermion  $\chi$  of mass  $m_\chi$  that can be identified with a bino in complete supersymmetric models. Finally, despite of being

allowed by gauge invariance, the single stop couplings to down-type quarks, as predicted in  $R$ -parity violating supersymmetry, are ignored for simplicity. We model all considered interactions by the Lagrangian

$$\mathcal{L}_3 = D_\mu \sigma_3^\dagger D^\mu \sigma_3 - m_3^2 \sigma_3^\dagger \sigma_3 + \frac{i}{2} \bar{\chi} \not{\partial} \chi - \frac{1}{2} m_\chi \bar{\chi} \chi + \left[ \sigma_3 \bar{t} (\tilde{g}_L P_L + \tilde{g}_R P_R) \chi + \text{h.c.} \right],$$

where we denote the strengths of the stop couplings to the fermion  $\chi$  by  $\tilde{g}$  and  $P_{L,R}$  are the left- and right-handed chirality projectors.

Aiming to precision predictions at the NLO accuracy, a renormalization procedure is required in order to absorb all ultraviolet divergences yielded by virtual loop-diagrams. This is achieved through counterterms that are derived from the tree-level Lagrangian by replacing all bare fields (generically denoted by  $\Psi$ ) and parameters (generically denoted by  $A$ ) by

$$\Psi \rightarrow Z_\Psi^{1/2} \Psi \approx \left[ 1 + \frac{1}{2} \delta Z_\Psi \right] \Psi \quad \text{and} \quad A \rightarrow A + \delta Z_A,$$

where the renormalization constants  $\delta Z$  are restricted in our case to QCD contributions at the first order in the strong coupling  $\alpha_s$ . Like in usual supersymmetric setups, the  $\tilde{g}$  couplings are of a non-QCD nature so that our simplified model does not feature new strong interactions involving quarks. The wave-function renormalization constant of the latter is therefore unchanged with respect to the Standard Model, contrary to the gluon one that must appropriately compensate stop-induced contributions. Adopting the on-shell renormalization scheme, the gluon and stop wave-function ( $\delta Z_g$  and  $\delta Z_{\sigma_3}$ ) and mass ( $\delta m_3^2$ ) renormalization constants read

$$\delta Z_g = \delta Z_g^{(SM)} - \frac{g_s^2}{96\pi^2} \left[ \frac{1}{\bar{\epsilon}} - \log \frac{m_3^2}{\mu_R^2} \right],$$

$$\delta Z_{\sigma_3} = 0 \quad \text{and} \quad \delta m_3^2 = -\frac{g_s^2 m_3^2}{12\pi^2} \left[ \frac{3}{\bar{\epsilon}} + 7 - 3 \log \frac{m_3^2}{\mu_R^2} \right],$$

where  $\delta Z_g^{(SM)}$  collects the Standard Model components of  $\delta Z_g$ . Moreover, we denote the renormalization scale by  $\mu_R$  and following standard conventions, the ultraviolet divergent parts of the renormalization constants are written in terms of the quantity  $1/\bar{\epsilon} = 1/\epsilon - \gamma_E + \log 4\pi$  where  $\gamma_E$  is the Euler-Mascheroni constant and  $\epsilon$  is linked to the number of space-time dimensions  $D = 4 - 2\epsilon$ .

The renormalization of the strong coupling is achieved by subtracting, at zero-momentum transfer, all heavy particle contributions from the gluon self-energy. This ensures that the running of  $\alpha_s$  solely originates from  $n_f = 5$  flavors of light quarks and gluons, and any effect induced by the massive top and stop fields is decoupled and absorbed in the renormalization constant of  $\alpha_s$ ,

$$\frac{\delta \alpha_s}{\alpha_s} = \frac{\alpha_s}{2\pi\bar{\epsilon}} \left[ \frac{n_f}{3} - \frac{11}{2} \right] + \frac{\alpha_s}{6\pi} \left[ \frac{1}{\bar{\epsilon}} - \log \frac{m_t^2}{\mu_R^2} \right] + \frac{\alpha_s}{24\pi} \left[ \frac{1}{\bar{\epsilon}} - \log \frac{m_3^2}{\mu_R^2} \right].$$

All loop-calculations achieved in this work rely on the OPP formalism. It is based on the decomposition of any loop amplitude in both cut-constructible and rational elements, the latter being related to the  $\epsilon$ -pieces of the loop-integral denominators ( $R_1$ ) and numerators ( $R_2$ ). For any renormalizable theory, there is a finite number of  $R_2$  terms, and they all involve interactions with at most four external legs that can be seen as counterterms derived from the tree-level Lagrangian [16]. Considering corrections at the first order in QCD, the  $\sigma_3$ -field induces three additional  $R_2$  counterterms with respect to the Standard Model case,

$$R_2^{\sigma_3^\dagger \sigma_3} = \frac{ig_s^2}{72\pi^2} \delta_{c_1 c_2} \left[ 3m_3^2 - p^2 \right],$$

$$R_2^{g\sigma_3^\dagger \sigma_3} = \frac{53ig_s^3}{576\pi^2} T_{c_2 c_3}^{a_1} (p_2 - p_3)^{\mu_1},$$

$$R_2^{gg\sigma_3^\dagger \sigma_3} = \frac{ig_s^4}{1152\pi^2} \eta^{\mu_1 \mu_2} \left[ 3\delta^{a_1 a_2} - 187\{T^{a_1}, T^{a_2}\} \right]_{c_3 c_4},$$

where  $c_i$ ,  $\mu_i$ , and  $p_i$  indicate the color index, Lorentz index, and the four-momentum of the  $i^{\text{th}}$  particle incoming to the  $R_2^{\dots}$  vertex, respectively. Moreover, the matrices  $T$  denote fundamental representation matrices of  $SU(3)$ .

Contrary to complete supersymmetric scenarios, the  $\tilde{g}$  operators present a non-trivial one-loop ultraviolet behavior that is not compensated by effects of other fields such as gluinos. Since we focus on QCD NLO corrections to the strong production of a pair of  $\sigma_3$  fields followed by their LO decays, the related counterterms are therefore omitted from this document.

Our stop simplified model has been implemented in FEYNRULES, and we have employed the NLOCT package to automatically generate all QCD ultraviolet and  $R_2$  counterterms (including the Standard Model ones). The output has been validated against our analytical calculations, which constitutes a validation of the handling of new massive colored states by NLOCT. Finally, the analytical results have been exported to a UFO module that we have imported into MADGRAPH5\_aMC@NLO. For our numerical analysis, we consider scenarios where  $m_3$  and  $m_\chi$  are kept free. The  $\tilde{g}_{L,R}$  parameters are fixed to typical values for supersymmetric models featuring a bino-like neutralino and a maximally-mixing top squark,

$$\tilde{g}_L = 0.25 \quad \text{and} \quad \tilde{g}_R = 0.06.$$

### III. BENCHMARK SCENARIOS FOR SGLUON HADROPRODUCTION

We construct a simplified model describing sgluon dynamics by supplementing the Standard Model with a real scalar field  $\sigma_8$  (a sgluon) of mass  $m_8$  lying in the adjoint representation of the QCD gauge group. Its strong interactions are described by gauge-covariant kinetic terms and we enable single sgluon couplings to quarks and gluons, like in complete models where such interactions are

$m_3$ [GeV]	8 TeV		13 TeV	
	$\sigma^{\text{LO}}$ [pb]	$\sigma^{\text{NLO}}$ [pb]	$\sigma^{\text{LO}}$ [pb]	$\sigma^{\text{NLO}}$ [pb]
100	$389.3^{+34.2\%}_{-23.9\%}$	$554.8^{+14.9\%+1.6\%}_{-13.5\%-1.6\%}$	$1066^{+29.1\%}_{-21.4\%}$	$1497^{+14.1\%+1.2\%}_{-12.1\%-1.2\%}$
250	$4.118^{+40.4\%}_{-27.2\%}$	$5.503^{+13.1\%+3.7\%}_{-13.7\%-3.7\%}$	$15.53^{+35.2\%}_{-24.8\%}$	$21.56^{+12.1\%+2.4\%}_{-12.3\%-2.4\%}$
500	$(6.594 \times 10^{-2})^{+45.5\%}_{-29.1\%}$	$(7.764 \times 10^{-2})^{+12.1\%+6.7\%}_{-14.1\%-6.7\%}$	$0.3890^{+39.6\%}_{-26.4\%}$	$0.5062^{+11.2\%+4.4\%}_{-12.8\%-4.4\%}$
750	$(3.504 \times 10^{-3})^{+48.8\%}_{-30.5\%}$	$(3.699 \times 10^{-3})^{+12.3\%+10.2\%}_{-14.6\%-10.2\%}$	$(3.306 \times 10^{-2})^{+41.8\%}_{-27.5\%}$	$(4.001 \times 10^{-2})^{+10.8\%+6.1\%}_{-12.9\%-6.1\%}$
1000	$(2.875 \times 10^{-4})^{+51.5\%}_{-31.5\%}$	$(2.775 \times 10^{-4})^{+13.1\%+15.5\%}_{-15.2\%-15.5\%}$	$(4.614 \times 10^{-3})^{+43.6\%}_{-28.3\%}$	$(5.219 \times 10^{-3})^{+10.9\%+7.9\%}_{-13.2\%-7.9\%}$
$m_8$ [GeV]	8 TeV		13 TeV	
	$\sigma^{\text{LO}}$ [pb]	$\sigma^{\text{NLO}}$ [pb]	$\sigma^{\text{LO}}$ [pb]	$\sigma^{\text{NLO}}$ [pb]
100	$3854^{+34.4\%}_{-24.1\%}$	$5573^{+14.9\%+1.6\%}_{-13.6\%-1.6\%}$	$10560^{+29.2\%}_{-21.5\%}$	$14700^{+13.6\%+1.2\%}_{-11.9\%-1.2\%}$
250	$38.89^{+41.3\%}_{-27.7\%}$	$54.32^{+14.5\%+3.9\%}_{-14.6\%-3.9\%}$	$150.4^{+35.7\%}_{-25.1\%}$	$214.5^{+12.9\%+2.5\%}_{-12.9\%-2.5\%}$
500	$0.5878^{+47.6\%}_{-30.0\%}$	$0.7431^{+15.8\%+7.6\%}_{-16.2\%-7.6\%}$	$3.619^{+40.8\%}_{-27.0\%}$	$4.977^{+13.3\%+4.7\%}_{-14.1\%-4.7\%}$
750	$(2.977 \times 10^{-2})^{+52.0\%}_{-31.9\%}$	$(3.353 \times 10^{-2})^{+17.2\%+12.1\%}_{-17.3\%-12.1\%}$	$0.2951^{+43.6\%}_{-28.4\%}$	$0.3817^{+14.0\%+6.9\%}_{-14.8\%-6.9\%}$
1000	$(2.328 \times 10^{-3})^{+55.9\%}_{-33.4\%}$	$(2.398 \times 10^{-3})^{+19.0\%+19.1\%}_{-18.4\%-19.1\%}$	$(3.983 \times 10^{-2})^{+46.1\%}_{-29.5\%}$	$(4.822 \times 10^{-2})^{+15.1\%+9.3\%}_{-15.6\%-9.3\%}$

TABLE I. Total cross sections for stop (upper panel) and sgluon (lower panel) pair production at the LHC, running at  $\sqrt{s} = 8$  and 13 TeV. Results are presented together with the associated scale and PDF (not shown for the LO case) uncertainties. Monte Carlo errors are of about 0.2-0.3% and omitted.

loop-induced. The corresponding effective Lagrangian reads

$$\mathcal{L}_8 = \frac{1}{2} D_\mu \sigma_8 D^\mu \sigma_8 - \frac{1}{2} m_8^2 \sigma_8 \sigma_8 + \frac{\hat{g}_g}{\Lambda} \sigma_8 G_{\mu\nu} G^{\mu\nu} + \sum_{q=u,d} \left[ \sigma_8 \bar{q} (\hat{g}_q^L P_L + \hat{g}_q^R P_R) q + \text{h.c.} \right],$$

where  $G^{\mu\nu}$  refers to the gluon field strength tensor and the single sgluon interaction strengths are denoted by  $\hat{g}$ . Although the  $\hat{g}$  operators induce single sgluon production, we ignore it in this work since the presence of a *complete* basis of dimension-five operators at tree-level is required to guarantee the cancellation, after renormalization, of all loop-induced ultraviolet divergences. We postpone the associated study to a future work.

The  $\hat{g}$  couplings being technically of higher-order in QCD (as in complete theories), the quark fields are renormalized like in the Standard Model. In contrast, the sgluon QCD interactions induce a modification of the on-shell gluon wave-function renormalization constant  $\delta Z_g$  and yield non-vanishing on-shell sgluon wave-function ( $\delta Z_{\sigma_8}$ ) and mass ( $\delta m_8^2$ ) renormalization constants,

$$\delta Z_g = \delta Z_g^{(SM)} - \frac{g_s^2}{32\pi^2} \left[ \frac{1}{\bar{\epsilon}} - \log \frac{m_8^2}{\mu_R^2} \right],$$

$$\delta Z_{\sigma_8} = 0 \quad \text{and} \quad \delta m_8^2 = -\frac{3g_s^2 m_8^2}{16\pi^2} \left[ \frac{3}{\bar{\epsilon}} + 7 - 3 \log \frac{m_8^2}{\mu_R^2} \right].$$

Sgluon effects are also subtracted, at zero-momentum transfer, from the gluon self-energy and absorbed in the renormalization of the strong coupling,

$$\frac{\delta \alpha_s}{\alpha_s} = \frac{\alpha_s}{2\pi \bar{\epsilon}} \left[ \frac{n_f}{3} - \frac{11}{2} \right] + \frac{\alpha_s}{6\pi} \left[ \frac{1}{\bar{\epsilon}} - \log \frac{m_t^2}{\mu_R^2} \right] + \frac{\alpha_s}{8\pi} \left[ \frac{1}{\bar{\epsilon}} - \log \frac{m_8^2}{\mu_R^2} \right].$$

They finally induce new  $R_2$  counterterms,

$$R_2^{\sigma_8 \sigma_8} = \frac{ig_s^2}{32\pi^2} \delta_{a_1 a_2} \left[ 3m_8^2 - p^2 \right],$$

$$R_2^{g \sigma_8 \sigma_8} = \frac{7g_s^3}{64\pi^2} f_{a_1 a_2 a_3} (p_2 - p_3)^{\mu_1},$$

$$R_2^{gg \sigma_8 \sigma_8} = \frac{ig_s^4}{384\pi^2} \eta^{\mu_1 \mu_2} \left[ 72(d_{a_1 a_4 e} d_{a_2 a_3 e} + d_{a_1 a_3 e} d_{a_2 a_4 e}) - 141 d_{a_1 a_2 e} d_{a_3 a_4 e} - 92 \delta_{a_1 a_2} \delta_{a_3 a_4} + 50(\delta_{a_1 a_3} \delta_{a_2 a_4} + \delta_{a_1 a_4} \delta_{a_2 a_3}) \right],$$

in the same notations as in the previous section.

We have implemented the sgluon simplified model in FEYNRULES and generated a UFO model that we have linked to MADGRAPH5\_aMC@NLO by means of the NLOCT package. The generated model has then been validated analytically against the above results. Our numerical study relies on benchmark scenarios inspired by an  $R$ -symmetric supersymmetric setup with non-minimal flavor violation in the squark sector [17], in which the only non-vanishing coupling parameters are fixed to

$$\frac{\hat{g}_g}{\Lambda} = 1.5 \cdot 10^{-6} \text{ GeV}^{-1},$$

$$(\hat{g}_u^{L,R})_{3i} = (\hat{g}_u^{L,R})_{i3} = 3 \cdot 10^{-3} \quad \forall i = 1, 2, 3.$$

#### IV. LHC PHENOMENOLOGY

In Tab. I, we provide stop and sgluon pair production cross sections for LHC collisions at center-of-mass energies of  $\sqrt{s} = 8$  and 13 TeV and for different mass choices. The results are evaluated both at the LO and NLO accuracy and presented together with the associated theoretical uncertainties. For the central values, we have

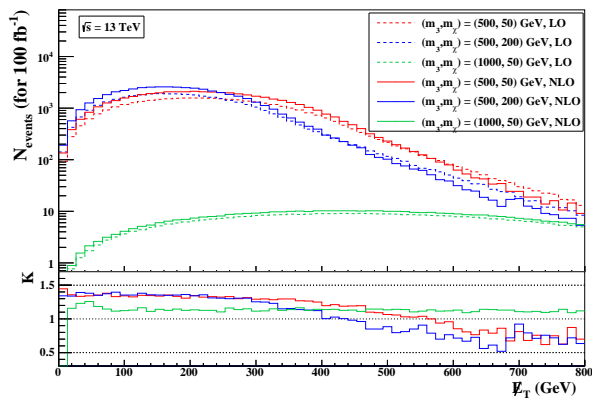


FIG. 1. Missing transverse energy spectrum for a stop pair production and decay signal. We consider several mass setups and show results at the NLO and LO accuracy (upper panel), together with their bin-by-bin ratio (lower panel).

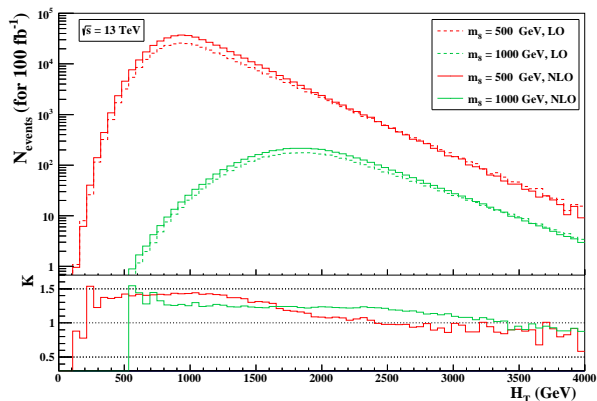


FIG. 2. Same as Fig. 1 for the  $H_T$  spectrum of sgluon signals.

fixed the renormalization and factorization scales to the stop/sgluon mass and used the NNPDF 2.3 parton distributions [18]. Scale uncertainties have been derived by varying both scales by a factor of two up and down, and the parton distribution uncertainties have been extracted from the cross section values spanned by the NNPDF density replica.

The results of Tab. I have been confronted to predictions obtained with the public packages PROSPINO [19] (stop pair production) and MADGOLEM [20] (sgluon pair production). Stop-pair total production rates have been found to agree at the level of the numerical integration error, while virtual and real contributions to sgluon-pair production are agreeing separately at the amplitude level. We have additionally performed independent calculations of the loop contributions based on FEYNARTS [21], that we have found to agree with our predictions.

Realistic descriptions of LHC collisions require to match hard scattering matrix elements to a modeling of QCD environment. To this aim, we make use of the MC@NLO method [22] as implemented in MADGRAPH5\_aMC@NLO. We match in this way the hard scattering process to the PYTHIA 8 parton showering

and hadronization [23], after employing the MADSPIN and MADWIDTH programs to handle stop and sgluon decays. Jet reconstruction is then performed by means of the anti- $k_T$  algorithm with a radius parameter set to 0.4 [24], as included in the FASTJET program [25], and events are finally analyzed with the MADANALYSIS 5 package [26]. Normalizing the results to an integrated luminosity of  $100 \text{ fb}^{-1}$ , we present, in Fig. 1, the distribution of a key observable for stop searches, namely the missing transverse energy. We show LO and NLO predictions for 13 TeV collisions as calculated by MADGRAPH5\_aMC@NLO in the context of three benchmark scenarios for which  $(m_3, m_\chi) = (500, 50) \text{ GeV}$  (red),  $(1000, 50) \text{ GeV}$  (green) and  $(500, 200) \text{ GeV}$  (blue). Similarly, we describe the hadronic activity  $H_T$  associated with the production of a sgluon pair in Fig. 2 in the case of a sgluon mass of 500 GeV (red) and 1000 GeV (green)<sup>1</sup>.

## V. CONCLUSIONS

In this Letter, we have demonstrated that a joint use of the FEYNRULES, NLOCT and MADGRAPH5\_aMC@NLO programs enables the full automation of the Monte Carlo simulations of high-energy physics collisions at the next-to-leading order accuracy in QCD and for non-trivial extensions of the Standard Model. This has been illustrated with simplified models such as those used for supersymmetry searches at the LHC. In this context, we have adopted setups that exhibit extra colored particles and non-usual interaction structures and presented the analysis of two exemplary signals with the automated tool MADANALYSIS 5.

In the aim of an embedding within experimental software, we have designed a webpage, <http://feynrules.irmp.ucl.ac.be/wiki/NLOModels> where hundreds of differential distributions are available for validation purposes, together with the associated FEYNRULES and UFO models.

## ACKNOWLEDGMENTS

We are extremely grateful to D. Goncalves-Netto, D. Lopez-Val and K. Mawatari for their help with MADGOLEM. We also thank R. Frederix, S. Frixione, F. Maltoni, O. Mattelaer, P. Torrielli and M. Zaro for enlightening discussions. This work has been supported in part by the ERC grant 291377 *LHCtheory: Theoretical predictions and analyses of LHC physics: advancing the preci-*

<sup>1</sup> With the current level of precision of the experimental searches, the current limits on the stop and sgluon masses, that are extracted on the basis of NLO total rates but LO simulations for the distributions, can be assumed to hold. Evaluating the NLO effects on the shapes and how this translates in terms of a modification of the limits goes beyond the scope of this work.

sion frontier, the Research Executive Agency of the European Union under Grant Agreement PITN-GA-2012-315877 (MCNet) and the Theory-LHC-France initiative of the CNRS/IN2P3. CD is a Durham International Ju-

nior Research Fellow, the work of VH is supported by the SNF with grant PBELP2 146525 and the one of JP by a PhD grant of the *Investissements d'avenir, Labex ENIGMASS*.

- 
- [1] H. P. Nilles, Phys.Rept. **110**, 1 (1984).  
 [2] H. E. Haber and G. L. Kane, Phys.Rept. **117**, 75 (1985).  
 [3] A. Salam and J. Strathdee, Nucl.Phys. **B87**, 85 (1975).  
 [4] P. Fayet, Nucl.Phys. **B113**, 135 (1976).  
 [5] C. Kilic, T. Okui, and R. Sundrum, JHEP **1002**, 018 (2010).  
 [6] J. Alwall, R. Frederix, S. Frixione, V. Hirschi, F. Maltoni, *et al.*, JHEP **1407**, 079 (2014).  
 [7] C. Degrande, (2014), arXiv:1406.3030 [hep-ph].  
 [8] A. Alloul, N. D. Christensen, C. Degrande, C. Duhr, and B. Fuks, Comput.Phys.Commun. **185**, 2250 (2014).  
 [9] J. Alwall, P. Schuster, and N. Toro, Phys.Rev. **D79**, 075020 (2009).  
 [10] D. Alves *et al.* (LHC New Physics Working Group), J.Phys. **G39**, 105005 (2012).  
 [11] C. Degrande, C. Duhr, B. Fuks, D. Grellscheid, O. Mattelaer, *et al.*, Comput.Phys.Commun. **183**, 1201 (2012).  
 [12] V. Hirschi, R. Frederix, S. Frixione, M. V. Garzelli, F. Maltoni, *et al.*, JHEP **1105**, 044 (2011).  
 [13] G. Ossola, C. G. Papadopoulos, and R. Pittau, Nucl.Phys. **B763**, 147 (2007).  
 [14] P. Artoisenet, R. Frederix, O. Mattelaer, and R. Rietkerk, JHEP **1303**, 015 (2013).  
 [15] J. Alwall, C. Duhr, B. Fuks, O. Mattelaer, D. G. Ozturk, *et al.*, (2014), arXiv:1402.1178 [hep-ph].  
 [16] G. Ossola, C. G. Papadopoulos, and R. Pittau, JHEP **0805**, 004 (2008).  
 [17] S. Calvet, B. Fuks, P. Gris, and L. Valery, JHEP **1304**, 043 (2013).  
 [18] R. D. Ball, V. Bertone, S. Carrazza, C. S. Deans, L. Del Debbio, *et al.*, Nucl.Phys. **B867**, 244 (2013).  
 [19] W. Beenakker, M. Kramer, T. Plehn, M. Spira, and P. Zerwas, Nucl.Phys. **B515**, 3 (1998).  
 [20] D. Goncalves-Netto, D. Lopez-Val, K. Mawatari, T. Plehn, and I. Wigmore, Phys.Rev. **D85**, 114024 (2012).  
 [21] T. Hahn, Comput.Phys.Commun. **140**, 418 (2001).  
 [22] S. Frixione and B. R. Webber, JHEP **0206**, 029 (2002).  
 [23] T. Sjostrand, S. Mrenna, and P. Z. Skands, Comput.Phys.Commun. **178**, 852 (2008).  
 [24] M. Cacciari, G. P. Salam, and G. Soyez, JHEP **0804**, 063 (2008).  
 [25] M. Cacciari, G. P. Salam, and G. Soyez, Eur.Phys.J. **C72**, 1896 (2012).  
 [26] E. Conte, B. Fuks, and G. Serret, Comput.Phys.Commun. **184**, 222 (2013).